ISSN 1330-3651 (Print), ISSN 1848-6339 (Online)
https://doi.org/10.17559/TV-20240422001483
Original scientific paper

# Impulse Shock Analysis of DMF Timing Ring in Vehicle Curb Crash Condition

Çağlar İMER, Mehmet Onur GENÇ*

**Abstract:** The design of the powertrain components by considering inertial properties is important for sustainability and lightness. The highest shock impulses cause the instant negative transient torque proportional to the system inertia and acceleration. In this study, the vehicle having the Double Mass Flywheel (DMF) system subjected to a specific curb obstacle is investigated experimentally in an urban driving profile. The LTI (Linear-Time-Invariant) system of the crash mechanism in vehicle systems is presented as one-dimensional and three-dimensional models. The free-body-diagram (FBD) is presented in the curb crash condition, and the obtained equation of motion is then correlated via curb crash analysis and experimental test results. The analysis is performed firstly in curb crash explicit analysis, then the system modeling with the mathematical powertrain model approach is obtained via one-dimensional modeling to find the effective impact torque on the timing ring. Then, the component-based design is analyzed and correlated with real experimental test results. The experimental Timing ring removal test is then correlated with the curb crash explicit model representing the full vehicle. Thus, the obtained minimum Timing Ring slipping torque presents the required urban safety DMF production process needs. The impulse shock analysis of DMF timing ring due to curb crashes is presented, and preventive methods are indicated by considering urban driving profile conditions.

**Keywords:** powertrain lightening; powertrain shock impulse; state-space model; system modeling; timing gear slipping torque

## 1 INTRODUCTION

Internal combustion engines with manual transmissions are operated in various working conditions. These conditions may have an impact on whole transmission components in terms of vibration, shock, over torque, and so on. It may cause any degradation of the transmission system which has the potential to cause any breakage, performance loss, or out-of-functional specifications. On the other hand, road conditions must be considered in the development of the whole system. One of the biggest issues in vehicles with manual transmission is that the impact torque phenomena occur in severe driving conditions. Some combination of ABS activation, obstacles on the road, and wrong downshift may create a resistive torque coming from the wheel to dual mass flywheel. Based on many parameters related to primary inertia, secondary flywheel inertia, other transmission component inertias, stiffness, engine calibration, ABS software, and hysteresis system, impact torque may reach ~20 - 40 times higher than engine mean torque. The lightening of the powertrain components is also important for sustainability including EOL (End-of-Life production) for the sub-components. Fig. 1 shows the general powertrain flow in a vehicle starting from the engine to the gearbox section. DMF provides inertial and damping properties to provide more robust and improved NVH (Noise, Vibration, and Harshness) performance.

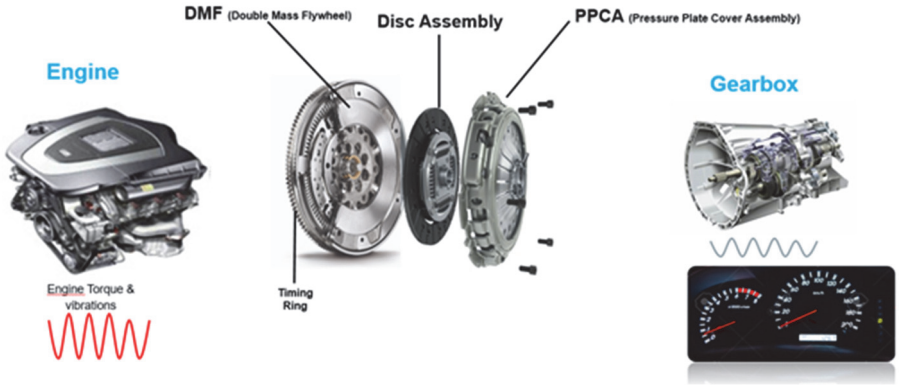


**Figure 1** Timing ring vs. DMF vs. powertrain visual chart

Torsional vibration of the automotive driveline has a significant influence on driving comfort. Moreover, impulse generation from road disturbances also should be considered an unpredictable damaging factor [1]. Many dynamic processes in the vehicle have different effects on the vibration. Therefore, a detailed coupling model is first established, considering the dynamics of the torsional vibrations of the driveline [2]. In industrial applications, the quarter and half-car models are generally considered for dynamic simulations. The models are used to analyze the influence of vehicle mass and suspension parameters on dynamic loads to provide requirements of dynamic loads generated when crossing over the considered obstacles [3]. The vehicle dynamic modeling strategy can be defined via State-Space representation well for the vehicle obstacle impact simulations [4]. The state space technique for the two-mass system can be also represented by the full-vehicle driveline model. The state-space system model definition method also provides the vehicle torsional vibration mathematical explanations [5].

In urban conditions, time domain and frequency domain processing methods are used to analyze vehicle body jerks, fluctuation of rotational speed, and torsional angle of the key components [6]. Wheel geometries and

vehicle mass properties meet the basic issues of the vehicle systems subjected to road obstacles [7]. Transient responses predicted by the driveline undergo severe torsional vibration and transmission gear rattle phenomenon [8]. For the torsional vibration and dependent shock impulse behavior of the curb crash, two-mass drive systems can be considered the simple representative model [9]. The importance of the vibration and dynamics of vehicle drive trains has increased because of noise and durability concerns [10]. Modern high-torque low-speed internal combustion engines (ICEs) generate torsional vibrations close in disturbance frequency to gearboxes' natural oscillation frequencies. Effective absorption of such oscillations requires a new torsional vibration damper between the internal combustion engine and gearbox design, which is implemented in the form of a dual-mass flywheel (DMF). One of the main reasons for DMF failure is its spring components destruction and the impact force generated on DMF system parts [11]. The dual mass flywheel (DMF) contains sub-system components such as an internal damper, hysteresis groups, and inertia ring providing vehicle ignition. Inertial characteristics of the sub-parts should be considered by both modal behavior and impulse shocks creating counter torque [12]. The impact force transferred into the driveline can be simulated via the equations of movement and 3D crashed analysis simulation study considering large obstacles creating damaging road surface response [13]. To represent the longitudinal vehicle dynamics of a front-wheel drive vehicle subjected to a curb crash, a simplified wheel can be composed with representative assigned mass, damping, and stiffness values, and powertrain model is generated [14]. The address of the first energy absorption step is the vehicle wheel over curb contact [15]. The simulation results show that the endurance and robustness of the powertrain components prevent the system from being damaged by unpredictable impulse shock. The design concerns for this phenomenon prolong the life of the mechanical components [16]. Fig. 2 explains the following flowchart in the study. DMF Production and Product Validation sections (Steps 1 and 2) explained in Section 2, and the interference between the Timing Ring and Primary Flywheel vs. Interference values are the main points investigated in the Timing Ring Slipping Torque phenomena. Step 3 shows the 3D model representing the curb crash, and the Driveline Equation of Motion to calculate the magnification ratio starting from Engine to Wheel modeled in Step 4. Step 5 indicates the discussions and decision steps for the flowchart.

Fig. 3 shows the representative Timing Ring damaged visually after the curb crash overcoming Timing Ring fitting torque. Due to excessive impact torque generation during curb crash, proportional to the Timing Ring inertia value the slipping torque overcomes the fitting torque value and the sliding occurs between the Primary Flywheel and Timing Ring. The interference fit is a form of fastening between two tight-fitting mating parts that produce a joint that is held together by friction after the parts are pushed together, fitting force between the timing ring/inertia ring and primary flywheel in this way. Considering the application radius of friction, a fitting torque of the timing ring can be calculated. The main target of this study is to optimize the minimum required interference fitting torque and to determine the generated impact torque on the system. Thus, the impact torque affecting the Timing Ring based on the driving profile is one of the important engineering approaches in vehicle systems using DMF.

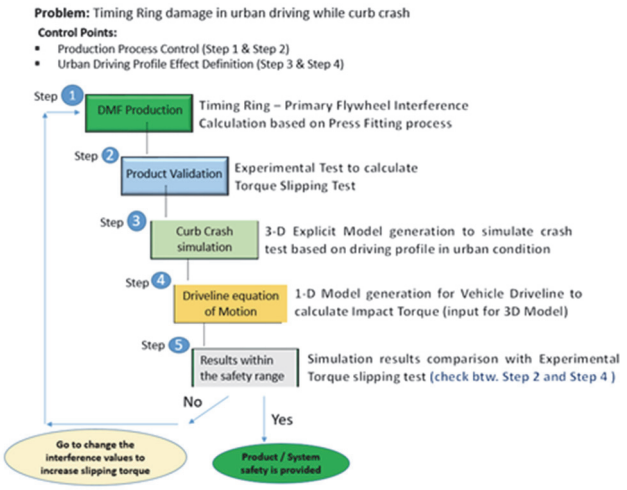


**Figure 2** Flowchart of the study-followed steps with explanations

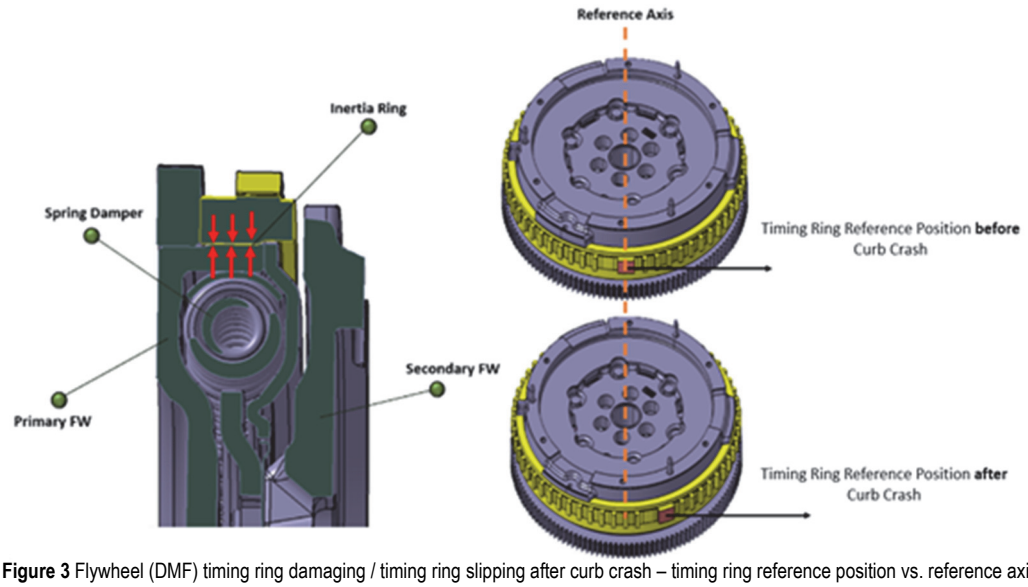


**Figure 3** Flywheel (DMF) timing ring damaging / timing ring slipping after curb crash – timing ring reference position vs. reference axis

## 2 TIMING RING MODEL

A timing ring has a function to manage the engine activation with a starter gear. Timing Ring gears are designed also by considering inertia effects both on mechanical endurance and NVH (Noise, Vibration, Harshness) concerns. The timing ring is assembled on the primary flywheel by using alternative methodologies well-known in the industry. The most preferable ones are press fitting in cold conditions, assembly without press load in hot conditions, or press fitting plus hot conditions. Another method is the welding of the ring on the primary flywheel. The main reason is to select the related method based on available process facilities of plants or product requirements. On the other hand, the material selection of the timing ring is another chapter during the development of the DMF. In this study, the primary flywheel material is DD14 and the timing ring is C35. In the case of low-grade material usage than C35 in severe applications, the timing ring can be deformed at high speed.

Based on many constraints in boundary conditions, material usage, and fitting method are crucial. To design reliable products, the optimization of the interference value of mating components vs generated impact torque on the flywheel should be studied during the development phase. In this study, interference fitting without welding and a friction coefficient of 0.1 were considered. Based on the FEA calculation, the slipping torque of the timing ring can be determined. The stiffness of the primary flywheel and timing ring has a big impact on changing the slipping torque of the flywheel. Fig. 4 shows the fitting FEA analysis of the designed DMF and interference values endured to slipping torque at ımpulse shock generated CCW (counter-clock-wise) torque [17]. In this FEA analysis, Primary FW is arranged with fixed support to provide slipping for the Timing Ring. The experimental test data pool of slipping torque tests from significant trials is correlated with FEA results as indicated in Fig. 4. The performed experimental tests are then tried to be correlated with FEA studies in the engineering approach. Thus, the new engineering designs for Timing Ring safety in the future can be estimated based on slipping torque value estimation. Fig. 5 shows the representative Timing Ring Removal (Slipping Torque) Measurement test bench. The obtained slipping torque value is used for FEA correlation and the comparison with the curb crash FEA explicit test.

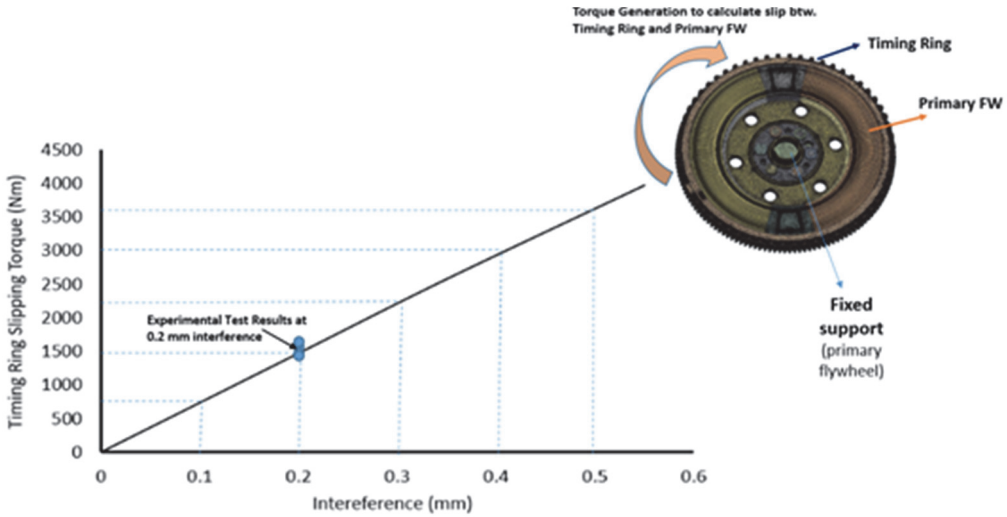


**Figure 4** FEA results correlated with experimental slip test-interference vs. timing ring slipping torque [17]

**Figure 5** Representative DMF timing ring slipping torque machine

## 3 SIMULATION METHODS

### 3.1 Crash Model

In this section, the FEA model representing the Crash analysis is investigated and analyzed. The explicit method is selected due to the investigated model having dynamic and time-dependent effects. In the model, the vehicle explained in Tab. 1 is assigned as the representative to the wheel 3D model with real weight to simulate crash occurrence at the curb with 50 km/h, 60 km/h, 70 km/h velocities. These velocities are selected within frequently urban speed conditions and used gears. A hexahedron mesh type is used in whole models; due to less notch existence one mesh type is selected. The obtained impulse value from the 3D Crash model is the input for the Driveline Model explained in 3.2.

### 3.2 Driveline Model

This section includes the details of the driveline modeling and sub-system information. Tab. 1 explains the vehicle system information related to resultant DMF damage caused by curb crashes in urban traffic conditions. The vehicle mass is considered fully loaded to simulate the worst-case scenario. The inertial effect of the curb crash interested in the $I_X$ inertia axis during the longitudinal

driving condition (Fig. 6). Tab. 2 shows the representative driveline ratio of the powertrain system generating power flow from the engine to wheels, conversely in case the impulse shock force generates from wheel to backward accordingly. Tab. 1 and Tab. 2 are used as system modeling input data for Vehicle Crash-Impulse Shock Representation investigated in Section 4. Each sub-part and system information given in these tables is used within the 1-D model constructed in Matlab.

**Table 1** Vehicle representative parameters used in the study

| | Parameter Value |
|---|---|
| Vehicle Mass - loaded / kg | 1740 |
| $I_X$ Inertial Value (loaded) / $\mathrm{kg \cdot m^2}$ | 1051 |
| Tire Radius / m | 0.30 |
| Engine Torque / Nm | 220 Nm |
| Inertial Proportion on Engine Crankshaft + Primary FW + Timing Ring | Engine Crankshaft: 35%<br>Primary FW: 45%<br>Timing Ring: 20% |

**Table 2** Global driveline ratio values of the vehicle system

| Gear °N | Gear Ratio | Differential Ratio | Global Ratio |
|---|---|---|---|
| Gear 1 | 45/10 | 58/15 | 17.4 |
| Gear 2 | 40/12 | 58/15 | 12.86 |
| Gear 3 | 40/25 | 58/15 | 6.17 |
| Gear 4 | 36/30 | 58/15 | 4.63 |
| Gear 5 | 32/40 | 58/15 | 3.08 |

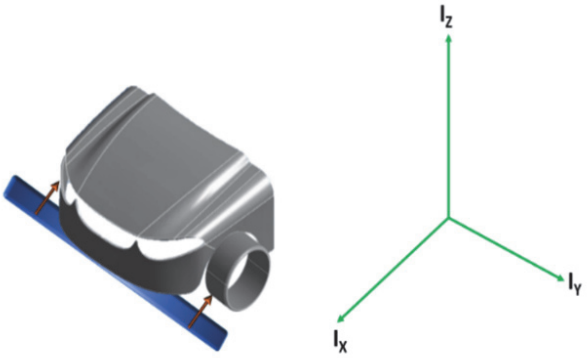


**Figure 6** Vehicle inertial effect based on global coordinate system

Eq. (1) and Eq. (2) define the equation of the impulse phenomenon. Eq. (1) explains the momentum change based on mass ($m$) and velocity ($v$) definitions. Impulse is explained in Eq. (2). Impulse is the rate of change in the momentum by considering the unit of time. $F$ indicates the impulse force occurring within the restricted time.

$$\Delta M = m_1 v_1 - m_2 v_2 \tag{1}$$

$$\Delta M = F \Delta t \tag{2}$$

As indicated in Fig. 7, from engine to wheel, an internal combustion engine, dual mass flywheel, clutch, gearbox, differential, half shafts, and wheels are presented in the main elements of the system. The stiffness of the flywheel, inertia, and damping characteristics of each element have a major influence on system response. As an input of the driveline model, impulse shock is extracted at the moment of the wheel crushing to an obstacle. Impulse can be identified as the change of momentum in the time domain.

Eq. (3) is the Newtonian mechanics equation that represents the force-generated torque ($T$) equation. The equation consists of the driveline equation of motion and includes the longitudinal inertia $J(\mathrm{kg \cdot m^2})$ in the $I_X$ direction referred from global coordinate systems (Fig. 6). $C(\mathrm{Nm \cdot s/rad})$ represents the damping of the related sub-system, and $k(\mathrm{Nm/rad})$ is the stiffness of the related driveline part. Based on the equation, the full powertrain system is represented in the Matrix form following. $\Theta$ represents the angular displacement of the rotated parts. Also, the matrix equations are the base of the State-Space representation of the modeled system Eq. (4).

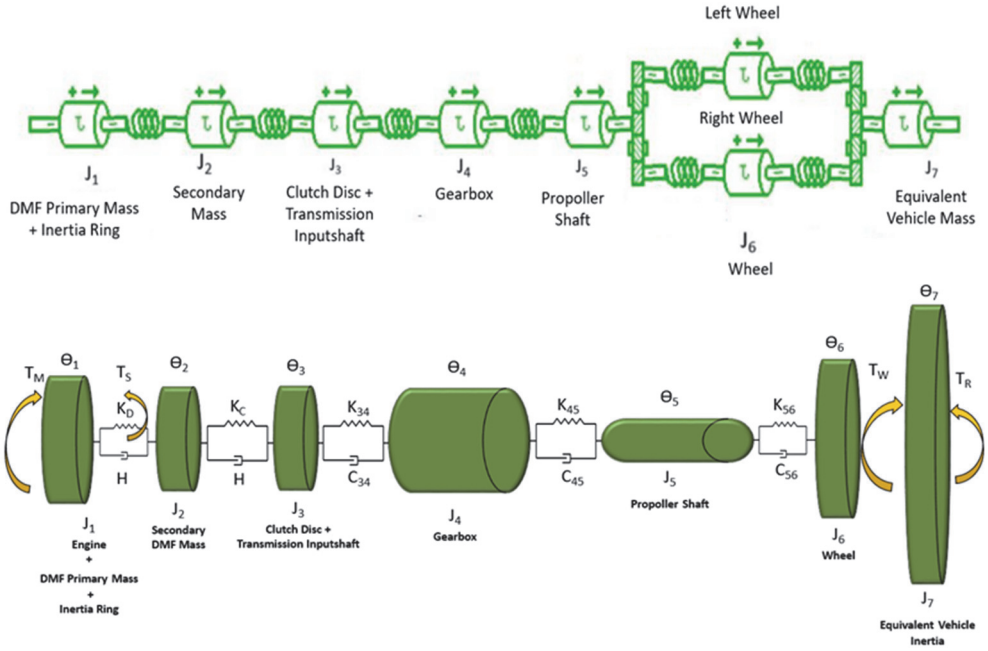


**Figure 7** Driveline power-transmission flow / AMESim system model

$$T\left(\mathrm{Nm}\right) = J_i \ddot{\theta} C_i \dot{\theta} k_i \theta \tag{3}$$

$$J\begin{bmatrix} J_1 & 0 & 0 & 0 & 0 & 0 & 0 \\ 0 & J_2 & 0 & 0 & 0 & 0 & 0 \\ 0 & 0 & J_3 & 0 & 0 & 0 & 0 \\ 0 & 0 & 0 & J_4 & 0 & 0 & 0 \\ 0 & 0 & 0 & 0 & J_5 & 0 & 0 \\ 0 & 0 & 0 & 0 & 0 & J_6 & 0 \\ 0 & 0 & 0 & 0 & 0 & 0 & J_7 \end{bmatrix}$$

$$C\begin{bmatrix} 0 & 0 & 0 & 0 & 0 & 0 & 0 \\ 0 & 0 & 0 & 0 & 0 & 0 & 0 \\ 0 & 0 & C_{34} & -C_{34} & 0 & 0 & 0 \\ 0 & 0 & -C_{34} & C_{34}+C_{45} & -C_{45} & 0 & 0 \\ 0 & 0 & 0 & -C_{45} & C_{45}+C_{56} & -C_{56} & 0 \\ 0 & 0 & 0 & 0 & -C_{56} & C_{56} & 0 \\ 0 & 0 & 0 & 0 & 0 & 0 & 0 \end{bmatrix}$$

$$k\begin{bmatrix} 0 & 0 & 0 & 0 & 0 & 0 & 0 \\ 0 & 0 & 0 & 0 & 0 & 0 & 0 \\ 0 & 0 & k_{34} & -k_{34} & 0 & 0 & 0 \\ 0 & 0 & -k_{34} & k_{34}+k_{45} & -k_{45} & 0 & 0 \\ 0 & 0 & 0 & -k_{45} & k_{45}+k_{56} & -k_{56} & 0 \\ 0 & 0 & 0 & 0 & -k_{56} & k_{56} & 0 \\ 0 & 0 & 0 & 0 & 0 & 0 & 0 \end{bmatrix}$$

$$\theta = \begin{bmatrix} \theta_1 \\ \theta_2 \\ \theta_3 \\ \theta_4 \\ \theta_5 \\ \theta_6 \\ \theta_7 \end{bmatrix}$$

$$T = \begin{bmatrix} T_M - T_S \\ T_S - T_C \\ T_D \\ 0 \\ 0 \\ -T_W \\ T_W - T_R \end{bmatrix}$$

## 4 VEHICLE CRASH-IMPULSE SHOCK REPRESENTATION

In the powertrain, two types of loads are considered to provide reliable systems. One of both is the drive load which is created by the internal combustion engine to accelerate and push the car forward. Another one is the coast load which decelerates the car. Coast load in the powertrain can be generated by the sum of the aerodynamic, rolling, and slope resistance. In this study, the main focus is to characterize the road load in case of any crossing an obstacle.

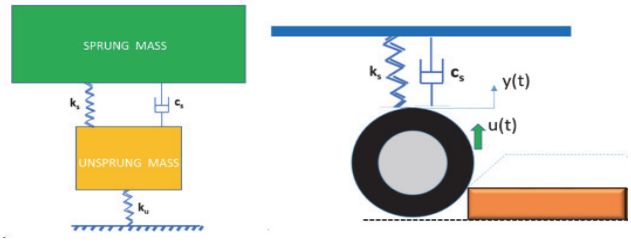


**Figure 8** Road obstacle & suspension dynamics

Other contributors to road loads were eliminated due to less effectiveness than the obstacle. During the rotation of the wheel, the wheel is in contact with the horizontal road surface. Rotation is always the horizontal surface till the wheel bumps into obstacles. However, at the moment of crashing the wheel with the obstacle, the friction point suddenly moves from the ground to the obstacle. This sudden change in road profile affects the reaction forces coming from the road which increases the coast load on the powertrain. The impact of the crush case was investigated with explicit analysis in the simulation. Representative vehicle load in the vertical axis and tire stiffness were considered in the crush analysis. Fig. 8 shows the suspension base vehicle parts of the system. Sprung mass corresponds to the car body supported by the suspension system, conversely unsprung mass explains the mass of the system parts that are not supported by damping and stiffness elements of the suspension system. $x$, $k$, $C$ and $v$ represent in order; Contact Depth (m), Spring Stiffness (N/m), Damping Coefficient $(\mathrm{N}\cdot\mathrm{sec/m})$, and Compression Speed (m/sec).

As indicated in Fig. 9, the front tires of the vehicle come in contact with an obstacle illustrated. Obstacle height was considered 0.15 m in the calculation. The related severe curb height is considered the most destructive curb design and is subjected at Gear 3 over 50 km/h to 70 km/h speed range in urban driving conditions [18]. FR represents the Impulse of the impact force at the curb crash moment. FCCW explains the counter-clock-wise force resulting in CCW (counter-clock-wise) torque impact shown as TCCW in Fig. 9. This phenomenon also can be named as negative torque having damaging results through impulse shock effect (Eq. (1), Eq. (2)).

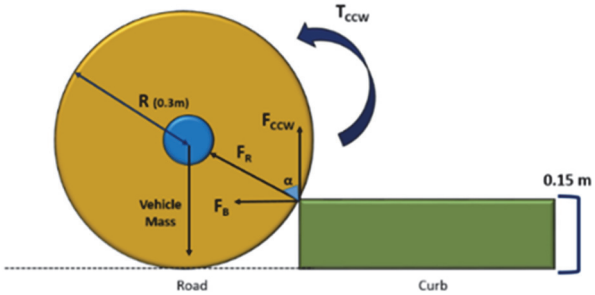


**Figure 9** Curb crash FBD impact reaction force vs. counter-clock-wise (CCW) torque generation

State-space representation is one of the important system definition tools for system modeling. In this section, the State-Space model is created to simulate the driveline modeling generated with data obtained from Tab. 1 and Tab. 2. Simulink Function creation is the main block to create the driveline model. Eq. (3) is the driveline equation of motion written as matrices form subjected to a time limiter

block. Eq. (3) in this block is written as a State-Space model to provide the system dynamic behavior. In this method, the derivatives of the selected states are observed and calculated in LTI (line time-invariant) state output. In this method, $\dot{x}$ represents the target state derivation, $\boldsymbol{A}$ stands for the state matrix, and $\boldsymbol{B}$ represents the input matrix. $\dot{y}$ is the output vector, including the $\boldsymbol{C}$ matrix as output, and the $\boldsymbol{D}$ matrix as feed-forward allowing system input to affect output directly Eq. (4).

$$\begin{aligned} \dot{x} &= [A][X]+[B][U] \\ \dot{y} &= [C][X]+[D][U] \end{aligned} \tag{4}$$

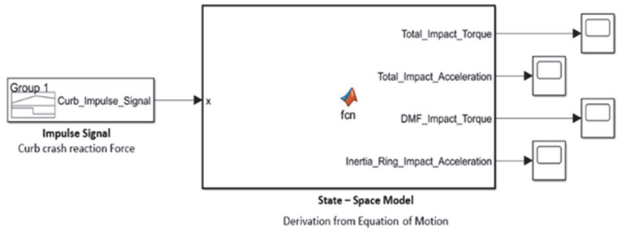


**Figure 10** Impulse force excited driveline system model

The state-space representation in system modeling is used in this study to create a control environment of the Driveline method. Fig. 10 shows the Matlab-Simulink System modeling representation. Impulse signal is created to represent the FCCW generated by FR explaining reaction force at curb crash. FR, which represents impulse force, is the input for the State-Space model of the Driveline equation of motion (Fig. 7). The outputs of the model are divided into total impact torque, total impact acceleration, DMF Impact torque representing primary FW, and Timing ring/Inertia ring impact torque.

## 5 ANALYSIS AND DISCUSSIONS

In this section, the results are discussed based on the developed methodology. The vehicle is represented via tire by assigning the same inertia and mass properties as in the real vehicle. Also, the obtained impulse value is the input of the Matlab model (Fig. 7) which correlates the transient impact torque affecting the DMF group. Fig. 11 is the chart of the curb crash model performed in the ANSYS explicit module. Explicit analysis considers and solves the model by considering the mass with the forward Euler method. The model is defined into the wheel to represent the total mass with an equal IX inertial value. The curb is defined with 0.15 m height to represent the urban damaging DMF effect at 3rd gear with 50 km/h, 60 km/h, and 70 km/h. The obtained value is calculated via FR impact force to FCCW to have impact torque affecting the Engine, DMF Primary FW and Timing Gear indicated in Fig. 7 and Eq. (3). The explicit analysis is performed considering the total 0.1 second crash duration at the curb, and the impulse signal is obtained between 0.03 second to 0.04 second.

Fig. 12 shows the obtained impact force values creating the Impulse phenomenon, which is the input signal of the TCCW damaging torque on Engine Cranks, DMF Primary FW, and timing ring to be used in the Driveline model as input. The analysis is performed at three different speeds at 3rd gear representing the most used urban driving ranges. The impulse values are obtained respectively 245 kN at 50 km/h, 272 kN at 60 km/h, and 445 kN at 70 km/h. The force increase shows the severity of non-optimal curb design danger as Impulse shock creation on powertrain components.

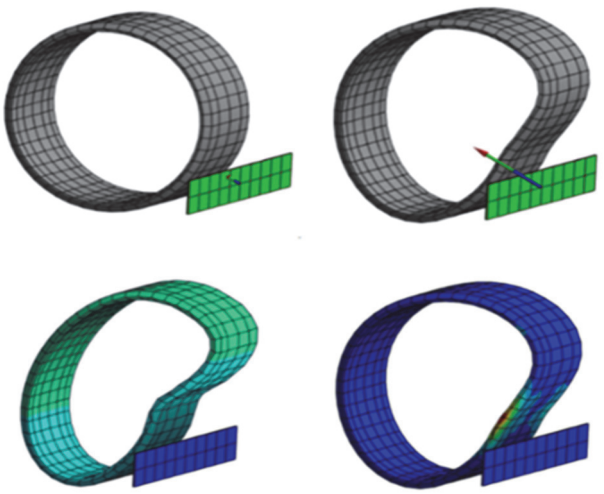

**Figure 11** Explicit model of representative vehicle model subjected to curb crash (input data for matlab model)

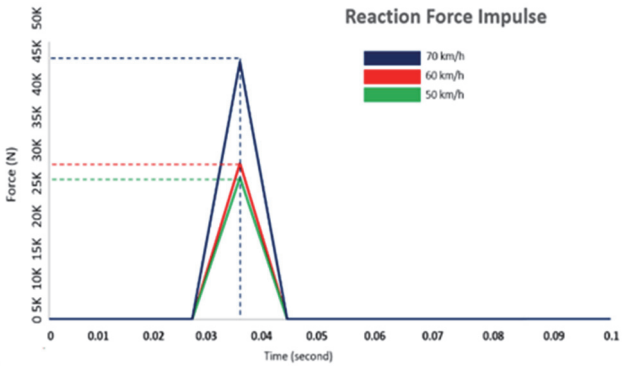


**Figure 12** Explicit model of representative vehicle subjected to curb crash at 50 km/h, 60 km/h, 70 km/h

Fig. 13 explains the experimental relative speed measurement between the Primary (blue curve) and Secondary Flywheel (red curve) at the curb crash [17]. Primary flywheel and secondary flywheel (Fig. 3) are assembled via damper springs ($k$) and hysteresis ($c$) parts Eq. (3). As shown in experimental measurement during curb crash due to counter-clockwise torque (Fig. 9) the Secondary Flywheel (Fig. 3) is forced by impulse shock and the impact torque causes resultant DMF timing ring damage. During the instant curb crash time range, the repetitive counter impact torque creates the negative directed force on damper springs and hysteresis groups. This case study explains also the importance of correct damper and hysteresis selection in DMF design. Fig. 13 shows the importance of considering the Timing Ring slipping torque definition accuracy while designing the DMF design.

Tab. 3 shows the obtained results as $F_R$ and $F_{CCW}$ vs. required minimum fitting torque of the timing ring affected by the Impulse shock phenomenon. The calculation of the minimal fitting torque should be considered with an empirical safety factor, which is the result of process and

design optimization of the timing ring to the DMF fitting process. In this study, the safety factor calculation is not investigated. In future studies, based on the obtained data the safety factor approach will be investigated. The process control for Fitting Value (btw. Timing Ring and Primary FW) vs. Slipping Torque has significant importance. The main reason is that the friction coefficient is not stable due to the assembly process, roughness, and shape deviation of components. Variation of the friction coefficient will be studied in further studies. Based on friction coefficient variability, a safety factor is recommended for timing ring slippage torque. In Tab. 3, the results show that the DMF timing ring obtained 1273 Nm impact torque caused via FR impulse at 50 Km/h. Under this torque level, the timing ring cannot endure in case a severe curb crash occurs (Fig. 9). As explained in Tab. 1, the timing ring is affected by 20% of the total impact torque due to covering 20% of the total inertia in Engine and DMF region represented with $J_1$ in Fig. 7. The global ratio for the 3rd gear is also the main factor for the obtained value in the equation of motion (Tab. 2, Eq. (3)). Similarly, at 60 km/h and 70 km/h the required minimum fitting torque is found respectively 1410 Nm and 2324 Nm. For this driving profile scenario, 2324 Nm is found the minimum Slipping Torque design to provide urban driving profile safety.

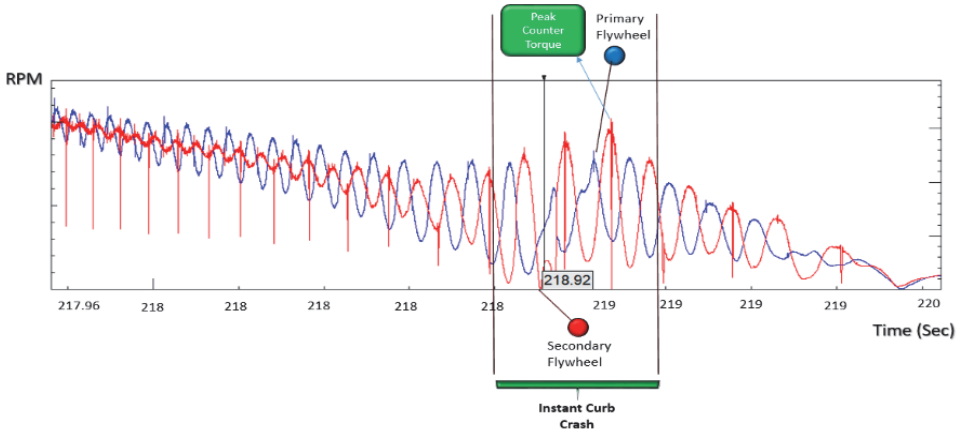


**Figure 13** Relative speed between primary and secondary flywheel [17]

**Table 3** Impact torque at 3rd gear acc. to speed vs. required min. fitting

| Speed (Urban most frequently used speeds) | Impulse Force on the Wheel (N) 3D Crash Test Results | CCW Resulting Force on the Wheel (N) Direct Impact Torque from 3D Model Affecting Wheel | Impact CCW Torque Effected on Timing Ring (Nm) 1D Driveline Model Results | Required Min. Slipping Torque of Timing Ring (Nm) Required minimum slipping torque w/o safety factor |
|---|---|---|---|---|
| 50 km/h | 245 K | 131 K | 1273 | > 1273 |
| 60 km/h | 272 K | 145 K | 1410 | > 1410 |
| 70 km/h | 445 K | 239 K | 2324 | > 2324 |

## 6 CONCLUSIONS

In this study, the vehicle representing the *C* segment is investigated during severe curb crash conditions by considering timing ring impact torque on the double mass flywheel (DMF). The impact force at the curb crash moment is represented via one-dimensional (1D) and three-dimensional (3D) models. The impulse shock effect over the curb on the road creates transient impact torque also called counter-clock-wise torque generation. This transient impact torque affects the powertrain system parts according to inertial proportion. The timing ring is part of the Engine crank and DMF Primary FW, and due to negative torque flow global ration makes an increasing impact torque on this powertrain system block. A damaging timing ring creates operating problems such as car stops, powertrain system damage, and car ignition failures. Through the study, an experimental approach is used and the methodology is proposed considering the urban driving profile probably subjected to severe curb crash at 3rd gear and the speeds respectively at 50 km/h, 60 km/h, and 70 km/h with explicit FEA methodology. For this reason, the Crash Model is firstly designed via the explicit method to find the impact torque factor, the vehicle is represented via a tire model and subjected to a crash test in explicit form. Afterward, the obtained impact torque value is used in the Driveline model to find the impact torque affecting the Timing ring proportional to the Engine-Primary FW-Timing Ring block. Thus, the powertrain system is modeled via the State-Space model, and then the Matlab mathematical model is created. Then, the obtained numerical results are presented to provide minimum DMF Timing Ring Slipping Torque. According to the investigated scenario in the study, based on the vehicle properties (Tab. 1) the minimum slipping torque is found based on variable curb crashing speeds at 50 km/h, 60 km/h and 70 km/h considering without safety factor consideration. Obtained results indicate the timing ring fitting process's importance and make an analytical requirement to prevent damage overcoming timing ring fitting torque. The presented methodology contributes to the impulse shock phenomenon by designing a powertrain system to estimate unpredictable road disturbances damaging the DMF timing ring.

## Acknowledgments

The authors gratefully thank for the research funding support to Valeo Automotive Systems.

## 7 REFERENCES


[1] Qu, J., Shi, W., Wang, J., & Chen, Z. (2022). Modeling and Analysis of Clutch Nonlinear Behavior in an Automotive Driveline for Suppressing Torsional Vibration. *Machines, 10*(819). https://doi.org/10.3390/machines10090819

[2] Hao, D., Zhao, C., & Huang, Y. (2018). A Reduced-Order Model for Active Suppression Control of Vehicle Longitudinal Low-Frequency Vibration. *Shock and Vibration, 2018*(5731347). https://doi.org/10.1155/2018/5731347

[3] Dargužis, A., Sapragonas, J., & Pilkauskas, K. (2011). Dynamic processes of a vehicle moving over step-shaped obstacles. *Journal of Vibroengineering, 13*(3), 536-543.

[4] Zhang, Y., Zhou, T., Yang, X., Wang, L., & Zang, M. (2019). Transient dynamic behavior of tire traversing obstacles in full vehicle scenario. *Journal of Automobile Engineering, 1*(13). https://doi.org/10.1177/0954407019871758

[5] Shahgholian, G., Shafaghi, P., Zinali, M., & Moalem, S. (2009). State Space Analysis and Control Design of Two-Mass Resonant System. *Second International Conference on Computer and Electrical Engineering,* 97-101. https://doi.org/10.1109/ICCEE.2009.105

[6] Zhong, B., Deng, B., & Zhao, H. (2019). Simulation Model and Method for Active Torsional Vibration Control of an HEV. *Applied Sciences, 34*(9). https://doi.org/10.3390/app9010034

[7] Dižo, J., Blatnický, M., Sága, M., Harušinec, J. G., & Legutko, S. (2020). Development of a New System for Attaching the Wheels of the Front Axle in the Cross-Country Vehicle. *Symmetry, 12*(1156). https://doi.org/10.3390/sym12071156

[8] Wu, H. & Wu, G. (2016). Driveline Torsional Analysis and Clutch Damper Optimization for Reducing Gear Rattle. *Shock and Vibration.* https://doi.org/10.1155/2016/8434625

[9] Nalepa, R., Najdek, K., Wróbel, K., & Szabat, K. (2020). Application of D-Decomposition Technique to Selection of Controller Parameters for a Two-Mass Drive System. *Energies, 13*(6614). https://doi.org/10.3390/en13246614

[10] Hua, X. & Gandee, E. (2021). Vibration and dynamics analysis of electric vehicle drivetrains. *Journal of Low Frequency, Noise, Vibration and Active Control, 40*(3), 1241-1251. https://doi.org/10.1177/1461348420979204

[11] Kindratskyy, L. R. & Osmak, O. (2022). Influence of Vehicle Acceleration Intensity on Dual-Mass Flywheel Elements and Transmission Load. *Transport Technologies, 3*(1), 65-76. https://doi.org/10.23939/tt2022.01.065

[12] Chen, L., Zhang, X., Yan, Z., & Zeng, R. (2019). Matching Model of Dual Mass Flywheel and Power Transmission Based on the Structural Sensitivity Analysis Method. *Symmetry, 11*(187). https://doi.org/10.3390/sym11020187

[13] Kropáč, O. & Múčka, P. (2008). Effect of obstacles in the road profile on the dynamic response of a vehicle. *Proceedings of IMechE, Part D, Journal of Automobile Engineering, 222*(3), 353-370. https://doi.org/10.1243/09544070JAUTO387

[14] Ötkür, M., Atabay, O., & Ereke, İ. M. (2017). Model-Based Predictive Engine Torque Control for Improved Driveability. *Journal of Polytechnic, 20*(1), 71-82.

[15] Michal, M. & Miloš, M. (2020). Reduction of Crankshaft Stress by Using The Torsional Vibration Damper. *Journal of Mechanical Engineering, 70*(2), 117-132. https://doi.org/10.2478/scjme-2020-0025

[16] Chen, K., Hu, J., & Peng, Z. (2016). Analysis of torsional vibration in an electromechanical transmission system. *Advances in Mechanical Engineering, 8*(6), https://doi.org/10.1177/1687814016650582

[17] Valeo Technical Documentation, Valeo Automotive Systems. (2013 - 2023). Valeo Automotive Systems, Turkey.

[18] Blagojevic, I., Vorotovic, G., Stamenkovic, D., Petrovic, N., & Rakıcevic, B. (2017). The Effects of Gear Shift Indicator Usage on Fuel Efficiency of a Motor Vehicle. *Thermal Science, 21*(1), 707-713. https://doi.org/10.2298/TSCI160806233B

[19] Hu, J., Yang, Y., Jia, M., Guan, Y., Fu, C., & Liao, S. (2020). Research on Harmonic Torque Reduction Strategy for Integrated Electric Drive System in Pure Electric Vehicle. *Electronics, 9*(1241). https://doi.org/10.3390/electronics9081241

[20] Yakut, O., Eren, H., Kaya, M., Oksuztepe, E., Polat, M., Omac, Z., Bekler, D., Kurum, H., & Celenk, M. (2013). Dynamic Risk Modeling for Safe Car Parking in Climbing over Urban Curbs. *International Conference on Connected Vehicles and Expo (ICCVE) 2013,* Nevada, USA. https://doi.org/10.1109/ICCVE.2013.6799837



**Contact information:**

**Çağlar İMER**, Product Technical Manager, Dual Mass Flywheel Expert
Research & Development Center,
Valeo Automotive Systems,
16245, Osmangazi, Bursa, TURKEY
E-mail: caglar.imer@valeo.com

**Mehmet Onur GENÇ**, Assistant Professor
(Corresponding Author)
Department of Mechatronics Engineering,
Bursa Technical University,
16310, Yıldırım, Bursa, TURKEY
E-mail: onur.genc@btu.edu.tr